

The local surface energy balance of the Ecology Glacier, King George Island, Antarctica: measurements and modelling

RICHARD BINTANJA

Institute for Marine and Atmospheric Research Utrecht, Utrecht University, P.O. Box 80005, 3508 TA Utrecht, the Netherlands

Abstract: Meteorological measurements performed during the austral summer of 1990–91 are used to evaluate the surface energy balance and ablation at an elevation of 100 m asl on the Ecology Glacier, which is an outlet glacier of the main ice cap of King George Island, Antarctica. Strong, gusty westerly winds prevail, although occasional south-easterly winds from the Weddell Sea reach the island. Generally, the climate can be characterized as relatively warm and humid with mean summer temperatures well above 0°C. As a result, considerable ablation (0.75 m water equivalent per month) takes place in the lower parts of the Ecology Glacier. The surface energy balance and ablation are calculated using a model with input from meteorological data. In spite of the large amount of cloud (0.83), solar radiation provided most of the energy used for melting (70.3 W m⁻²). The longwave radiation, sensible heat flux and latent heat flux contributed -9.5, 27.4 and 7.4 W m⁻² respectively. Calculations show that a temperature rise of 1°C increases the ablation by almost 15%. This indicates that the ice caps and glaciers currently present on the subantarctic islands and the Antarctic Peninsula may be quite sensitive to climate change.

Received 17 October 1994, accepted 5 April 1995

Key words: Antarctica, King George Island, meteorology, surface energy balance, ablation

Introduction

King George Island, the largest island of the South Shetland Islands, is located at the northern tip of the Antarctic Peninsula (Fig. 1). Approximately 94% of the island is covered with ice. The highest point of the ice cap extends to about 650 m asl. Because of its northerly position (62°S), King George Island is located in the subantarctic westerly wind zone. Its climate can be characterized by a rapid succession of eastward moving low pressure systems, which transport relatively warm, humid air towards the coast of Antarctica. This is the cause of the relatively high values of the annual mean temperature (2.0°C) and humidity (82%) at Arctowski Station, situated on the south-eastern side of the island (Fig. 2) (Martianov & Rakusa-Suszczewski 1989). Fig. 3 shows the annual temperature cycle at Arctowski Station; it can be readily seen that temperatures higher than 0°C can occur throughout the entire year. During summer, the mean temperature is well above zero. Precipitation varies from 500 mm yr⁻¹ at sea-level (Martianov & Rakusa-Suszczewski 1989) to approximately 2000 mm yr⁻¹ at the summit (Zamoruyev 1972), which indicates that there is an extremely large vertical precipitation gradient of 2300 mm km⁻¹ (for comparison, Oerlemans (1992) uses a precipitation gradient of 1200 mm km⁻¹ for Nigaardsbreen, which is located in the wet climate of western Norway). The glacier equilibrium-line altitude lies at about 100 m asl. As a result, most of the glaciers terminate in ice-cliffs from which icebergs calve.

Located on the down-wind side of the island, Arctowski Station (Fig. 2) is more or less shielded from the direct effects

of the predominantly westerly winds. Because of the descending, relatively warm Föhn-like winds, the cloud amount on the south-eastern side is lower than on the north-western side of the island. As a result, more solar radiation reaches the surface on the south-east side, which further contributes to the warmer climate there. An interesting feature is the frequent occurrence of cold, south-easterly winds originating from the Weddell Sea area (Martianov & Rakusa-Suszczewski 1989). Due to the relatively warm climate of the South Shetland Islands and of the northern part



Fig. 1. Location of King George Island, South Shetland Islands.

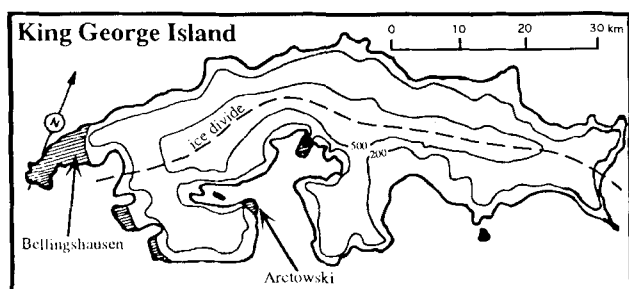


Fig. 2. Map of King George Island showing surface elevation contours in m. Ice-free areas are denoted by hatching. The location of two of the major research stations on the island, Arctowski and Bellingshausen, is indicated by arrows.

of the Antarctic Peninsula, significant ablation occurs at the lower parts of the ice caps and glaciers during summer. Therefore, the ice masses in this area are probably quite sensitive to changes in temperature. Since small ice caps react relatively fast to climate changes and because the amount of ice in these areas seems to be considerable, their potential effect on sea-level changes should not be disregarded. The fact that the Antarctic Peninsula area is located in the marginal sea-ice zone, which may be one of the regions most sensitive to climate change (Manabe & Stouffer, 1980, Mitchell *et al.* 1990), amplifies the potential effect of these regions on sea-level changes. The potential rapid decline of the small subantarctic ice caps is totally opposite to the response of the main Antarctic ice sheet, which is assumed to

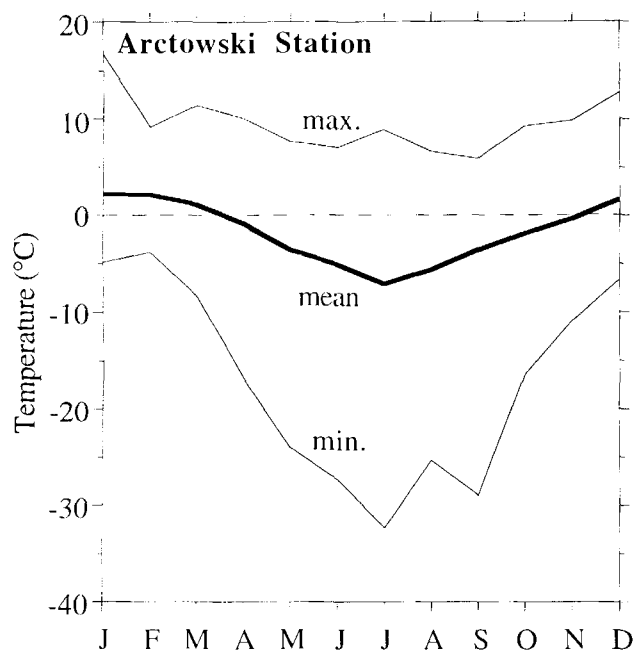


Fig. 3. Mean annual cycle of the air temperature at Arctowski Station averaged over the years 1978-1987 (Martianov & Rakusa-Suszczewski 1989). Also shown are the absolute extreme values for this period.

increase its mass as a result of short-term global warming because the increase in precipitation outweighs the increase in ablation (Huybrechts & Oerlemans 1990). Few studies have been done on the mass balance of the ice caps of the South Shetlands and other subantarctic islands. A summary of mass balance measurements on the South Shetlands is given by Orheim & Govorukha (1982). Hogg *et al.* (1982) present the summer surface energy balance of Hodges Glacier on South Georgia. They conclude that radiation and sensible heat flux provide about equal amounts of the energy used for ablation. Glacial geological evidence of quaternary glaciations in the Antarctic Peninsula area is given by Clapperton & Sugden (1988) and Clapperton (1990). They conclude that during the last 100 000 years the glaciers in this region have fluctuated synchronously with glaciers elsewhere in the southern hemisphere.

The present experiment was carried out during December 1990-January 1991 within the framework of the First Dutch Antarctic Expedition to Arctowski Station, King George Island. Among the 19 scientists attached to this expedition were three meteorologists who carried out a glaciological/meteorological experiment on the nearby Ecology Glacier (Fig. 4). This paper focuses on the surface energy balance and mass balance at one specific site on this glacier. In this paper, the measurements are presented and compared with model results.

Instrumentation

The experimental set-up is depicted in Fig. 4. Two meteorological stations were operative during the period 17 December-16 January, one at site 1 on land and the other at site 2 on ice. Unfortunately, logistic problems prevented us from establishing two additional stations higher up the glacier, as was originally intended. In this paper, we present only results of measurements made at site 2.

Site 2 is located about 600 m from the calving edge of the Ecology Glacier at an elevation of 100 m asl. The meteorological station contained sensors to measure temperature (at 0.5, 2 and 6 m above the surface), relative humidity (0.5, 2, 6 m), wind speed (2, 6 m), wind direction (6 m) and shortwave incoming and reflected radiation (1.5 m). The temperature and humidity sensors were ventilated. The entire station stood freely on the surface, implying that the height of the sensors above the surface was reasonably constant throughout the experiment, even at this location with a high ablation rate. During the measuring period, the surface at site 2 remained reasonably flat with only a slight inclination ($\leq 2^\circ$) towards the south-west. All sensors were sampled every two minutes. Data were transmitted by radio almost every hour to the computer at Arctowski Station, where they were stored and analysed. In this way, a complete one-month data-set without breaks was obtained. For further information about the experimental set-up and data acquisition routine (see Bintanja *et al.* 1991).

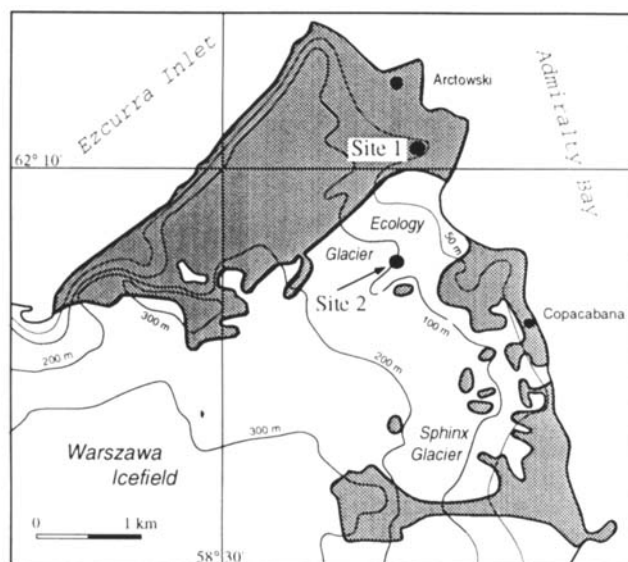


Fig. 4. Location of Arctowski Station, Ecology Glacier and the two measuring sites. Ice-free land is indicated by grey areas.

A cable balloon system was used near Arctowski Station to obtain vertical profiles of temperature, humidity, wind speed, wind direction and pressure in the lowest 1000–1500 m of the atmosphere. The number of soundings was limited to 23 as a result of frequent strong winds ($> 10 \text{ m s}^{-1}$) during which the cable balloon system could not be operated.

Cloud observations (amount, type and base height) were performed three times a day at Arctowski Station. During the experiment, several mass balance measurements (snow density–depth profiles, stake readings) were carried out near site 2. Additionally, some mass balance measurements were performed at other elevations on the Ecology Glacier.

Meteorological conditions

As stated above, the climate of King George Island is determined mainly by the rapid succession (2–3 days) of eastward moving cyclonic systems. As a result, the weather is extremely variable (during the experiment no specific weather type persisted for more than one day). Fig. 5 shows the variation in some meteorological quantities as measured at site 2. Of particular interest for the surface energy balance (and hence, the surface mass balance) is the large amount of cloud, which significantly reduces the solar radiation reaching the surface. Daily mean cloudiness never dropped below 0.59 (in fact, no entirely cloud-free sky was observed during the experiment). Usually, the cloud base height was about 300 m. The large variability in the incoming solar radiation at the surface indicates large variations in cloud optical depth.

The mean and the extreme meteorological conditions are listed in Table I. A comparison of these one-month averages with the 10 yr summer means as listed by Martianov & Rakusa-Suszczewski (1989) shows that the 1990–91 summer

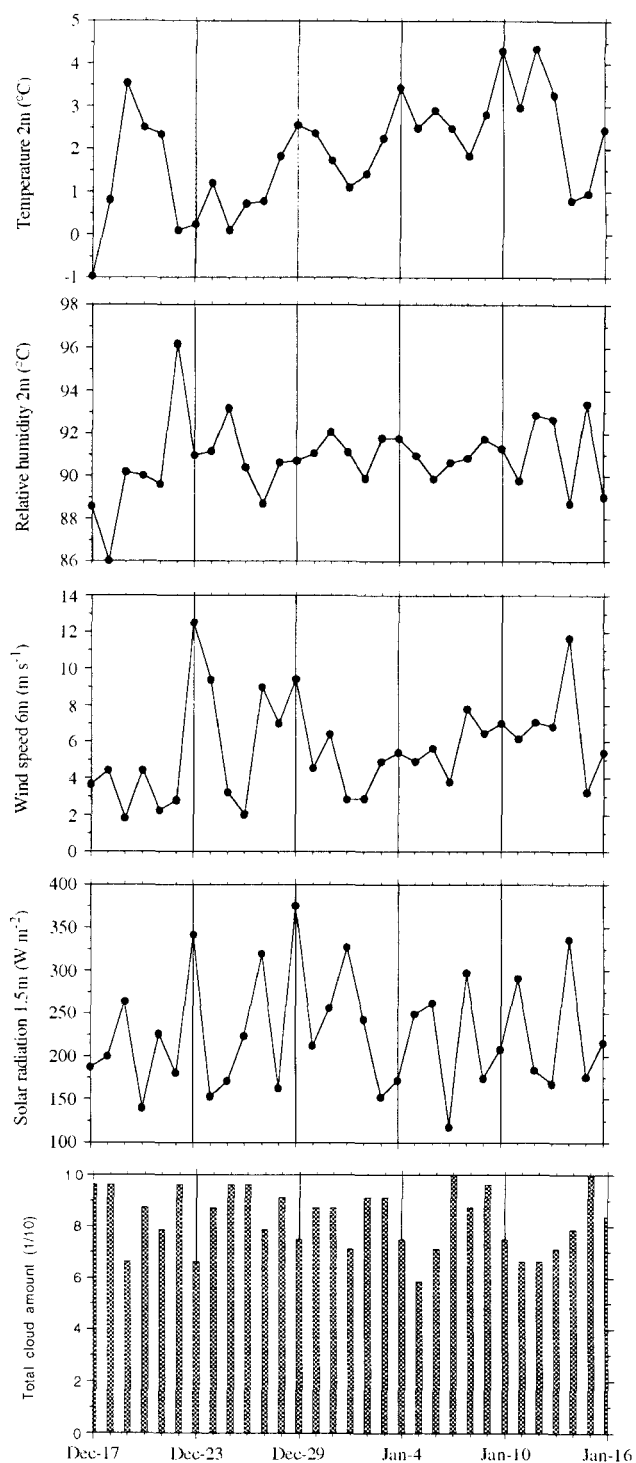


Fig. 5. Daily mean values of the meteorological quantities measured at site 2 for the period 17 December 1990 to 16 January 1991.

was approximately 1.5°C warmer than normal, whereas the other meteorological variables did not differ much from the 10 year means. This should be borne in mind when interpreting the energy balance and mass balance results. The mean daily cycle in wind speed and temperature is shown in Fig. 6.

Table I. Mean and extreme meteorological conditions at site 2 for the period 17 December to 16 January. Minimum and maximum values refer to hourly means except for cloud amount, where they refer to daily means.

Quantity	x	min	max
Temperature 2 m (°C)	1.9	-2.2	6.2
Relative humidity 2 m (%)	92	82	99
Wind speed 6 m (m s ⁻¹)	5.7	0.5	20.1
Cloud amount	0.83	0.59	1.00

Restricted by the presence of a melting surface, the diurnal variation of air temperature is only 1.2°C. In daytime, heating of the air over the glacier is probably enhanced by advection of air which is heated over the surrounding rocks and moraines. The diurnal variation of the wind speed shows an interesting peak during the night, which may indicate shallow nocturnal katabatic flows along the local slopes of the glacier. Indeed, during some nights with low synoptically forced winds, there were relatively strong, south-westerly (downslope) winds. However, these events occurred irregularly due to the frequent disturbance by large-scale weather systems.

The distribution of wind direction during the experiment is shown in Fig. 7a. The variation of wind speed with wind direction is shown in Fig. 7b. Obviously, westerly and north-westerly winds are most common. Winds from these directions occurred more than 50% of the time. These winds are also the strongest ones, which is a normal phenomenon in the subantarctic westerly wind zone. Winds from south-easterly directions are less common and much weaker.

Although the depression activity at King George Island is high, the precipitation rates at sea-level are quite low (barely 500 mm yr⁻¹ at Arctowski Station and up to 700 mm yr⁻¹ in the wind-exposed western part of the island). During the measuring period, 47 mm of precipitation was recorded at Arctowski Station of which 45 mm fell as rain and 2 mm as snow.

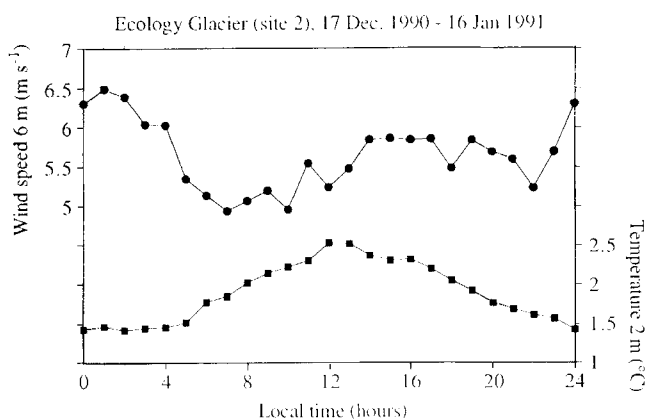


Fig. 6. Mean diurnal variation of wind speed at 6 m (circles) and temperature at 2 m (squares) at site 2 for the period 17 December 1990 to 16 January 1991.

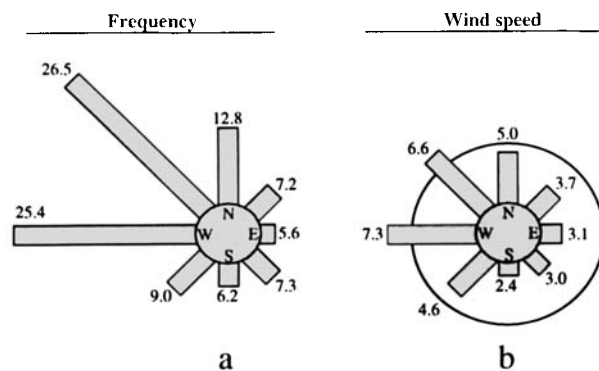


Fig. 7. a. Occurrence of wind direction (in % of time).
b. variation of wind speed (m s⁻¹) with wind direction. The circle indicates the period mean wind speed of 5.7 m s⁻¹. Based on hourly data at site 2 during the entire 31-day measuring period.

The 23 balloon soundings revealed that the average lapse rate in the lowest 1000 m was -6.2 K km⁻¹, which is considered to be a normal value for the well-mixed, relatively humid lowest layer of the atmosphere and almost equal to the moist-adiabatic lapse rate of -6.5 K km⁻¹.

Of specific interest are the relatively cold, south-easterly winds. Fig. 8 shows that the air temperature with winds from this direction is about 1°C lower than average. It is suggested that these winds originate from the Weddell Sea area (Parish 1983, Schwerdtfeger 1984): westward-moving cold, stable air masses in the lowest layers reach the mountain barrier of the Antarctic Peninsula (with altitudes up to 2000 m asl or more) and are deflected to the north. These winds are commonly referred to as barrier or inertial winds. Flowing to the north, the cold, stable air masses reach the Antarctic Sound and enter the Bransfield Strait where the barrier effect is absent. Eventually, these flows are able to reach the South Shetland Islands from the south-east, where their original characteristics (cold, stably stratified) can still be recognized.

Fig. 9 shows two soundings just before and after the inflow of a cold air mass from the south-east on 1 January. Weather maps show that on that day King George Island was situated in a weak high pressure ridge between two low pressure systems. At 09 h the air in the lowest km is moderately stable with winds from west to north. Six hours later, the wind has veered towards the east in the lowest layers. At the same time the potential temperature has dropped by 2°C, indicating advection of cold air in the lowest 500 m of the atmosphere. Also the stability increases significantly in this lowest layer. According to Martianov & Rakusa-Suszczewski (1989), these stable air masses are generally not able to flow over the crest of the King George Island ice cap and reach the north-western side of the island. At the south-eastern side of the island, however, the occurrence of these cold air masses tend to decrease the ablation.

Note that the low temperatures during winds from south-westerly directions (Fig. 8) may be connected to the

mentioned nocturnal katabatic winds.

Model description

One of the objectives of this study is to study the surface energy balance and relate it to the measured ablation. Since not all the components of the surface energy budget were measured directly, a model is used to calculate the complete surface energy balance. A further advantage of using a model is that it enables us to perform a sensitivity analysis. The model consists of a part in which all the surface-atmosphere fluxes are evaluated, coupled to a part in which the (sub-) surface temperatures, melting, densities and penetration of solar radiation are calculated. The entire model is the same as the one used by Bintanja (1992) and will be described below. The energy fluxes towards the surface in the direction normal to the surface can be written as:

$$S+L +H+LE+G=M \quad (1)$$

with S = the net shortwave radiation, L = the net longwave radiation, H = the sensible heat flux, LE = the latent heat flux, G = the conductive heat flux and M = the energy available for melt. Equation (1) is commonly referred to as the surface energy balance equation. The energy transport due to precipitation is neglected. The incoming and reflected solar radiative fluxes are measured directly. The emitted longwave radiation ($L\uparrow$) is evaluated from the calculated surface temperature (T_s) using $L\uparrow = \sigma T_s^4$ in which σ is Boltzmann's constant. The incoming longwave radiation is calculated using a broad-band emissivity model for the atmosphere with 20 layers in the vertical (the layer thickness increases with height). The absorbing and emitting gases taken into account in this radiative transfer model are water vapour, carbon dioxide and ozone. Clouds are assumed to radiate as black bodies while carbon dioxide is assumed to be well mixed with a mixing ratio of 350 ppmv. Observed temperature, relative humidity and lapse rate are used to define the vertical input profiles of temperature and water vapour in the lowest 1000 m (where most of the infrared radiation received at the surface comes from). Above 1000 m, the standard sub-arctic summer profiles of temperature, water vapour and ozone are used (McClatchey *et al.* 1971). Observations of cloud base height and lapse rate determine the cloud base temperature in the model.

The turbulent fluxes of sensible and latent heat are computed using the well-known Monin-Obukhov similarity theory. For the stably stratified surface layer, the stability correction functions are taken from Duynkerke (1991), which seem to be better fits to measured vertical profiles under very stable conditions. For the unstable case the expressions provided by Höglström (1988) are used. In order to be certain that the calculations are performed within the surface layer, values from the lowest level of measurement and the surface are used to evaluate the vertical gradients. This means that the calculated surface temperature and surface specific humidity

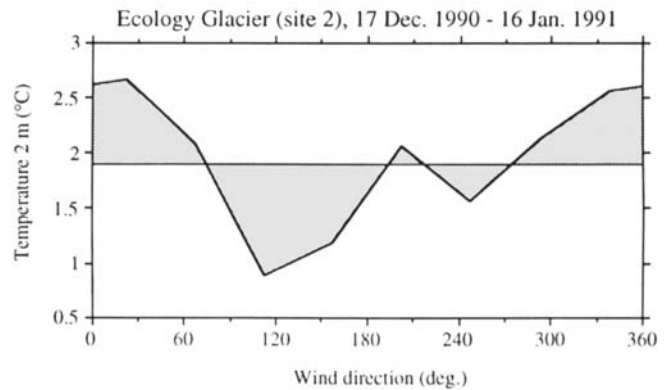


Fig. 8. Mean variation of air temperature (2 m) with wind direction during the measuring period at site 2, based on hourly wind direction and temperature data. Temperatures represent average values for wind direction intervals of 45°.

(evaluated assuming saturation with respect to ice) must be used. This also means that the surface roughness lengths need to be known. The roughness length for momentum (z_{0m}) can be estimated from the wind speed profile under near-neutral conditions. The resultant scatter is very large, which is obviously due to the inhomogeneous surface topography around site 2 (Fig. 4). Wind profile measurements at site 2 show that the best estimate of z_{0m} is 1.0×10^{-3} m, which seems to be a reasonable value for (wet) snow and ice surfaces (Paterson 1981, Hogg *et al.* 1982). Although the snow cover disappeared at the end of the measuring period and an obvious rougher ice surface became exposed, no attempt was made to correct for a non-constant value of z_{0m} . The roughness lengths of heat and moisture are commonly taken equal to z_{0m} if the roughness Reynolds number ($Re = z_{0m} u^*/\nu$) does not become too large (Garratt & Hicks 1973, Brutsaert 1982, Bintanja & Van den Broeke 1995). Since this is generally the case over smooth snow and ice surfaces, it is assumed here that the scalar roughness lengths are equal to z_{0m} .

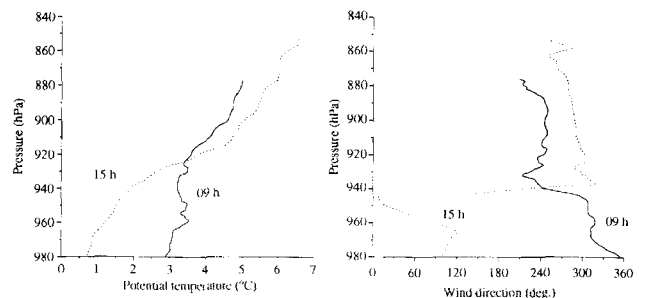


Fig. 9. Vertical profiles of potential temperature and wind direction at Arctowski Station just before (09h00) and after (15h00) the onset of a relatively cold, south-easterly wind on 1 January 1991. All curves were smoothed with a 5-point running mean.

In the uppermost layers of a glacier, horizontal advection and conduction of heat can be neglected. If the vertical velocity of the snow is neglected too, which is justified in our case with only small amounts of solid precipitation, the temperature distribution inside the snow/ice layers is governed by the following equation:

$$\rho c_p \frac{\partial T}{\partial t} = \frac{\partial}{\partial z} \left(K \frac{\partial T}{\partial z} \right) + \frac{\partial S_i}{\partial z} + \psi \quad (2)$$

in which ρ is the snow/ice density, c_p is the specific heat capacity at constant pressure, T is the snow/ice temperature, z is the vertical coordinate, K is the snow/ice conductivity, S_i the subsurface solar radiative flux and ψ the energy release by phase changes. Boundary conditions of Eq. (2) are given by the surface energy balance Eq. (1) and by zero conductive heat flux at the lower boundary. The conductivity K (in $\text{W m}^{-1} \text{K}^{-1}$) depends on the density (kg m^{-3}) as given by Paterson (1981):

$$K = 2.1 \times 10^{-2} + 4.2 \times 10^{-4} \rho + 2.2 \cdot 10^{-9} \rho^3 \quad (3)$$

The solar radiative flux inside the snow/ice is assumed to decrease exponentially with depth according to:

$$S_i = S e^{-\beta z} \quad (4)$$

where β is the extinction coefficient which is assumed to vary linearly with density:

$$\beta = \begin{cases} 10 \text{ m}^{-1} & \text{for } \rho = 400 \text{ kg m}^{-3} \\ 2.5 \text{ m}^{-1} & \text{for } \rho = 900 \text{ kg m}^{-3}. \end{cases}$$

The processes of melting, percolation of meltwater and refreezing are modelled as in the model of Greuell & Oerlemans (1987). The vertical distribution of temperature, density and liquid water content is evaluated in the snow layer (initially 114 cm thick) and in the top 50 cm of the underlying ice. If the temperature of a certain layer is at 0°C , any additional energy will be used for melting and the layer thickness decreases. Meltwater will remain in this layer until it exceeds 4% of the total layer mass (Harstveit 1984), then the layer is saturated with water. From a saturated layer any additional meltwater can percolate downwards where it can be taken up by a non-saturated layer or it can heat up a layer where the temperature is below 0°C due to refreezing. If this heating results in a temperature higher than 0°C in the model, the temperature is set equal to 0°C and the remaining amount of water that can stay there as liquid water is computed. If the meltwater reaches the ice surface, it is assumed to run off. The measured density profile at 16 December is used as initial snow-density profile and the density of ice is taken to be 900 kg m^{-3} . Obviously, the snow density can change according to the amount of liquid and refrozen water and snow inside a certain layer. The net ablation is the sum of run-off and sublimation/evaporation.

Equation (2) is solved on a stretched grid with grid distances ranging from 5–25 cm. The layer thickness in the model depends on the initial density profile in order to obtain a uniform density within each layer. The time step is 1 hr, the same as used for calculating the atmosphere-surface fluxes. Thus, each hour the model calculates the surface energy fluxes, the run-off, the (sub-) surface temperature distribution and the mass budget of each model layer. Note that all the surface fluxes except S and the incoming longwave radiative flux depend on the surface temperature, which itself is a prognostic variable in the model.

The surface energy balance

In this section the surface-atmosphere fluxes at site 2 on the Ecology glacier are discussed. They are calculated with the above described model for the entire measuring period (from 17 December 1990 to 16 January 1991). The variation in the daily mean surface fluxes for this period is shown in Fig. 10. Notice that the conductive heat flux at the surface (G in Eq. (1)) is not given since it is very small compared to the other fluxes. This is due to the fact that the (sub-) surface temperatures were nearly constant at 0°C during the entire period. As expected from the variability in the weather, there are large variations in the surface energy balance terms. Variations in the net solar radiation are due not only to variations in incoming solar radiation (Fig. 5), but also to variations in albedo, whose temporal variations are also quite large (Fig. 11). This is due to the accumulation of (small amounts of) fresh snow on 17 and 25 December, which raised the albedo to 0.85. In between, the melting snow cover had an albedo of 0.65–0.73. At the end of the measuring period the snow cover disappeared, revealing glacier ice partially covered by the remains of slush with an albedo of about 0.63.

The net longwave radiation is comparatively small and less variable. This is due to the frequent occurrence of low clouds which causes the temperature difference between cloud base and surface to be small. Occasionally, L even becomes larger than zero due to the presence of 'warm' clouds. Although it seems that clouds therefore enhance ablation, the net effect of clouds on total radiation is to cool the surface, which is indicated by the absence of the 'radiation paradox' (Ambach 1974). This means that the decrease in net shortwave radiation due to clouds is larger than the increase in net longwave radiation.

The sensible heat flux is directed towards the surface throughout almost the entire period, indicating stable conditions, as can be expected over a melting glacier. Due to the stable stratification, turbulence must be generated by shear stress since buoyancy diminishes the turbulent motions. Obviously, the temperature difference between atmosphere and glacier is also important for the value of H . For instance, during the storm of 23 December the sensible heat flux was very small due to the low temperatures (Fig. 5). On the other hand, the storm on 29 December advected relatively warm air

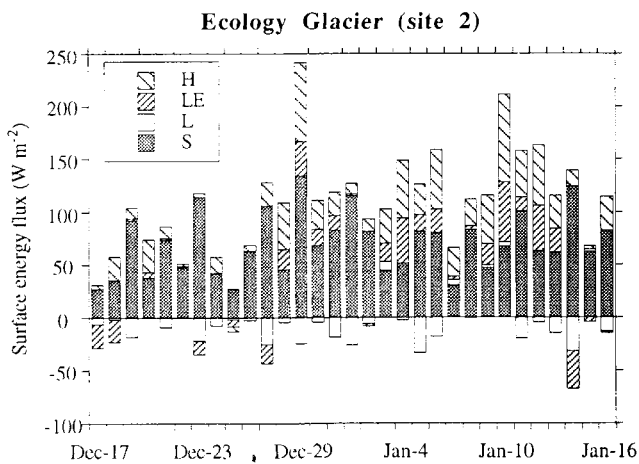


Fig. 10. The daily mean surface heat fluxes at site 2 as evaluated with the model for the period 17 December 1990 to 16 January 1991. Shown are net shortwave radiation (S), net longwave radiation (L), sensible heat flux (H) and the latent heat flux (LE). A positive value indicates a flux towards the surface.

of 2.5–3.0°C towards the glacier, which caused the sensible heat flux to be as high as 75 W m⁻².

The latent heat flux is mostly positive, indicating a transport of moisture towards the surface. On average, this is due to the warm and very humid air overlying the relatively cold, melting surface.

Table II summarizes the mean and extreme surface energy fluxes and albedo values. The apparent constancy of the incoming longwave radiative flux is noticeable. As stated above, this is due to the large amounts of low clouds. The very small negative value of the net longwave radiation causes the net radiation to be the largest contributor to the ablation (64%). The fluxes of sensible heat (29%) and latent heat (7%) are the other important contributors of energy used for melting. These values can be compared with the summertime surface energy balance results of Hogg *et al.* (1982) over Hodges Glacier, South Georgia. On the Ecology Glacier, the turbulent fluxes are less important in the total surface energy budget than on Hodges Glacier, where they provide 46% of the energy used for ablation, because the latter is situated in a warmer climate with mean summer temperatures of c. 4.5°C. The 1990–91 summer at Arctowski Station was relatively warm, as stated in section 3, so that during ‘normal’ years the downward transported turbulent energy may even be smaller.

The mean diurnal cycle of the surface energy fluxes is depicted in Fig. 12. Obviously, the variation of the radiative fluxes is reasonably smooth due to the averaging over 31 days. The mean diurnal variation in net longwave radiation is extremely small compared to that of the net shortwave radiation, for the reasons discussed above.

The mean diurnal cycle of the turbulent fluxes shows a maximum in the daytime at about 13h00–14h00, which is clearly connected to the diurnal temperature cycle. At night,

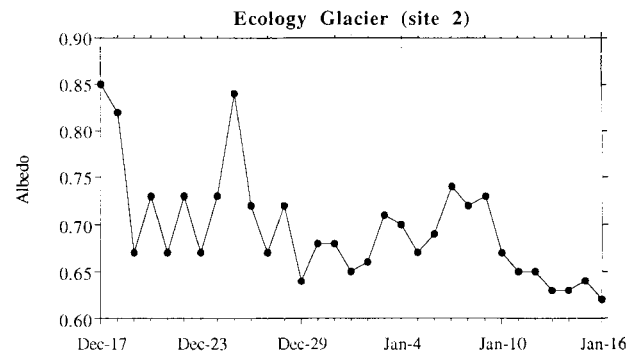


Fig. 11. The daily mean albedo as measured at site 2 for the period 17 December 1990 to 16 January 1991.

a secondary peak is apparent, which is due to the relatively high nocturnal wind speeds (Fig. 6). Apparently, during some nights there is a flow of cold air down the glacier, forced by cooling of the air due to a downward directed sensible heat flux. Thus, our data suggest that nocturnal katabatic winds may develop occasionally on the slopes of the Ecology Glacier during summer, although they have only a small effect on the surface energy and mass balance.

The surface mass balance

Surface mass balance measurements (snow density profiles and stake readings) were performed regularly at site 2. The mean density appears to be around 500 kg m⁻³, a value typical for wet snow. The snow density appears to be fairly constant throughout the measuring period.

Fig. 13a shows the cumulative modelled ablation and the measured values for the entire measuring period. The daily cycle in ablation can be recognized, which is due to the fact that solar radiation provides most of the energy for ablation. The total ablation is 73.5 cm water equivalent (w.e.) (measured) and 72.8 cm w.e. (modelled). The agreement between model and observation therefore seems to be very good. However, one should bear in mind that this is achieved by an appropriate choice of surface roughness lengths. Therefore, one could also interpret the good agreement

Table II. Mean and extreme surface energy balance terms (W m⁻²) and albedo for the period 17 December to 16 January. Minimum and maximum values refer to daily means.

	mean	min	max
Incoming shortwave	224.9	117.5	374.9
Reflected shortwave	-154.6	-87.0	-239.9
Net shortwave	70.3	27.3	133.9
Incoming longwave	305.5	282.3	323.7
Emitted longwave	-315.0	-310.9	-315.5
Net longwave	-9.5	-33.2	8.2
Net radiation	60.8	21.4	109.4
Albedo	0.69	0.62	0.85
Sensible heat flux	27.4	-4.7	83.2
Latent heat flux	7.4	-35.7	56.3

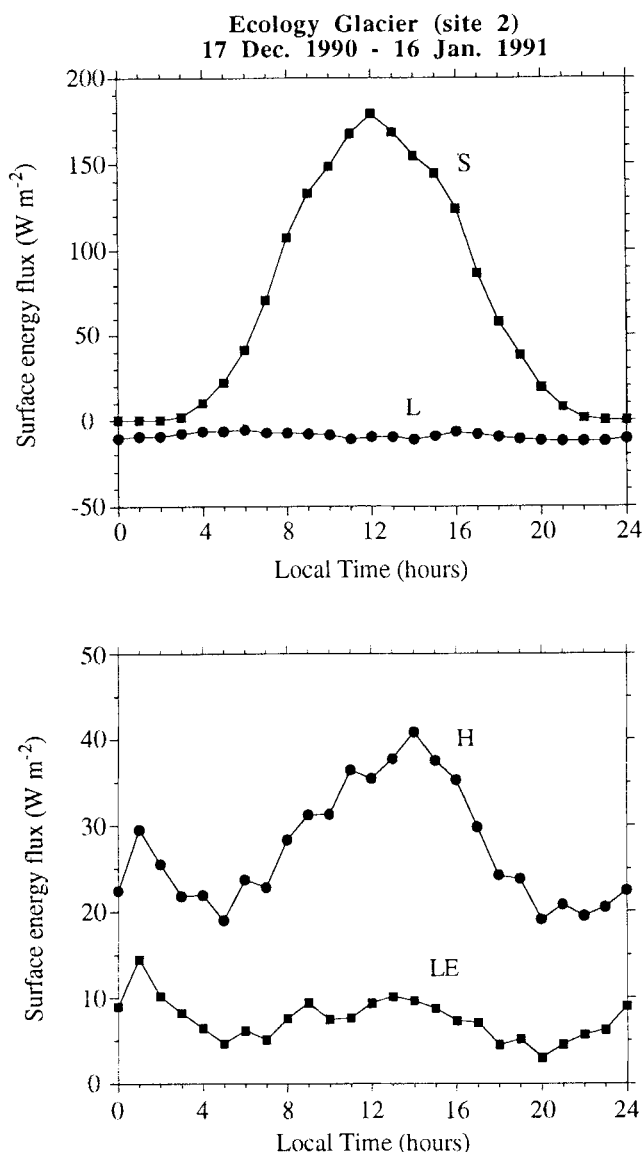


Fig. 12. Mean diurnal variation of net shortwave radiation (S), net longwave radiation (L), sensible heat flux (H) and the latent heat flux (LE) at site 2 for the period 17 December 1990 to 16 January 1991. A positive value indicates a flux towards the surface.

between measured and simulated ablation as an indication of the fact that the roughness lengths are correct. In the subsequent section the sensitivity of the ablation to changes in roughness lengths will be discussed. The height of the surface relative to the initial snow-ice interface is shown in Fig. 13b. The entire snow pack, which is initially 114 cm thick, is removed during the experiment. During the last few days, the model calculations indicate that ice-melt occurs, in accordance with the observations. The modelled thickness of the snow pack on 10 January is too small, as can be inferred from comparison with the measured thickness of about 30 cm. This obviously coincides with an overestimation of the cumulative ablation at this time.

A comparison of the modelled and the measured ablation for each 3–6 day period when the mass balance at site 2 was measured is shown in Fig. 14. Except for one period the agreement seems to be quite good. During the ‘bad’ period the model underestimates the ablation, which might be connected with the surfacing of the snow-ice boundary within this period. Snow-density measurements become very inaccurate when the snow depth has diminished to less than about 20 cm since the snow layer then is loaded with liquid water. Further, the spatial inhomogeneity in ablation and surface conditions on scales of a few metres becomes increasingly important when the snow depth decreases to about 20 cm or less. The surface then consists of a combination of meltwater pools, remains of slush and patches of snow, which makes it virtually impossible to relate the ablation calculated using data from the meteorological station to the ablation measured only a few metres away.

The surface temperature becomes $< 0^{\circ}C$ for only a limited time. Nevertheless, it is important to take into account these periods with regard to the ablation since energy subtracted from snow/ice layers during freezing conditions has to be resupplied to them when the surface energy balance becomes positive before melting starts. Therefore, the occurrence of freezing conditions during the night tempers daytime ablation.

Mass balance measurements performed at 200 m asl on the Ecology Glacier indicated that the ablation at that height was only 7.0 cm w.e. during a period when the ablation at site 2 was 52.5 cm w.e. Run-off at 200 m asl is severely hindered by the thick snow pack. This indicates that on the Ecology Glacier there is an extremely large mass balance gradient with height.

Sensitivity analysis

In order to gain insight into the robustness of the simulated surface energy balance terms and ablation rates a sensitivity analysis is performed. If a meteorological variable used as input is varied, this analysis also gives an indication of the sensitivity of the surface energy budget and ablation rates to variations in (local) climate. Some selected input variables and model parameters have been subsequently varied, after which the model calculates the ‘new’ surface energy balance terms and ablation rates for the entire measuring period in each case. The changes in surface energy balance terms are presented in Table III. Only the most prominent features of the changes are discussed below.

Clearly, a 10-fold change in the momentum roughness length (with the scalar roughness lengths remaining unchanged) has a drastic effect on the turbulent fluxes. A smaller z_{om} decreases the (downward directed) turbulent fluxes whereas a larger z_{om} increases the turbulent fluxes. However, the decrease in H and LE due to a smaller z_{om} is much less than the increase in the other case. This can be attributed to a feedback effect: a smaller z_{om} decreases the downward fluxes, which lowers the surface temperatures. This, in turn, en-

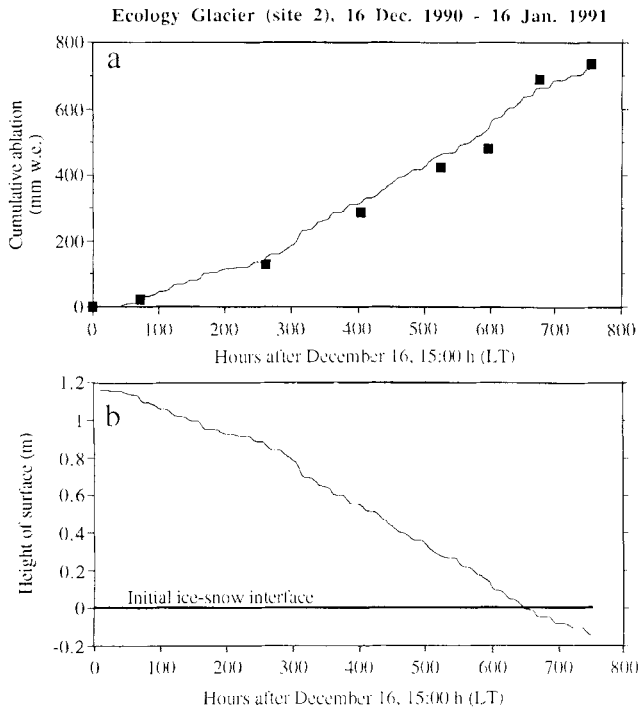


Fig. 13. a. Cumulative ablation and b. height of the surface with respect to the initial snow-ice interface as simulated with the model for site 2. Measured cumulative ablation values are indicated by the dots.

hances the surface–atmosphere temperature difference, which leads to higher fluxes (although the increased stability tends to diminish turbulence). Eventually, the turbulent fluxes have decreased only slightly. On the other hand, a larger z_{om} does not lead to significant warming of the surface since it is already 0°C for most of the time. Therefore, the temperature difference between surface and atmosphere cannot decrease and the turbulent fluxes become substantially larger.

A reduction in net solar radiation has only a minor effect on the magnitude of the surface fluxes. A change in incoming longwave radiation has a larger effect due to the fact that the net solar radiation is only 70.3 W m^{-2} , which is much smaller compared to the value of the incoming longwave radiation of 305.5 W m^{-2} . A reduction in incoming radiation cools the surface, which results in slightly larger turbulent fluxes.

An increase of 1°C in the air temperature increases the sensible heat flux by 58%. Note that the changing air temperature does not affect the moisture content of the air. This results in a small decrease in LE due to the increase in stability, which reduces the turbulent motions.

An increase in wind speed of 20% enhances the turbulent fluxes and warms the surface, a result that is to be expected. Finally, a change in the water holding capacity (WHC) of the snow layers has only a small effect on the surface heat fluxes. The largest changes occur when the presence of liquid water

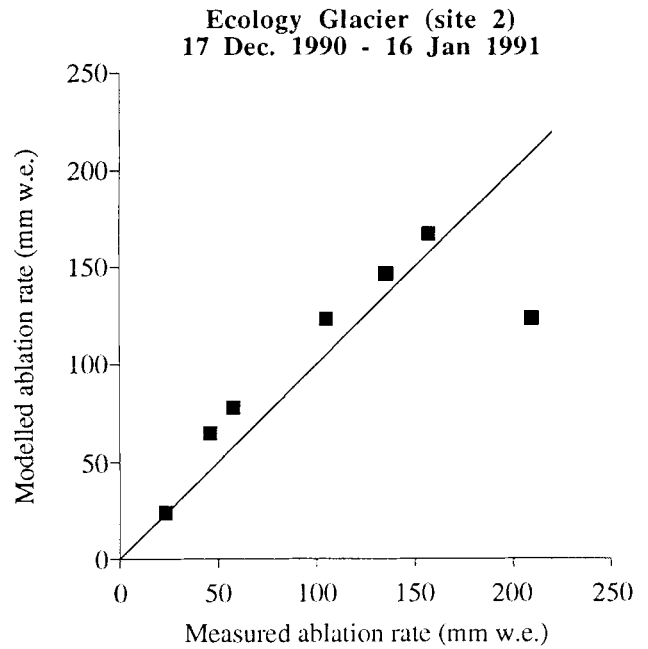


Fig. 14. Simulated versus measured ablation (mm w.e.) for seven 3–6 day periods at site 2.

in snow is omitted ($WHC = 0$). Then, the surface is colder due to the fact that the (sub-) surface layers are able to cool more quickly because of the absence of liquid water. A lower surface temperature leads to larger values of L_{\uparrow} , H_s and LE . The surface temperature with $WHC = 0$ is therefore equal to 0°C for a shorter period of time than for the reference experiment.

A general feature of the sensitivity experiments is that the variations in the turbulent fluxes (especially the sensible heat flux) are more pronounced than the changes in the radiative fluxes.

The change in ablation resulting from some of the perturbations made is shown in Fig. 15. Indeed, more or less

Table III. Change in surface energy balance terms (W m^{-2}) with respect to the mean values for the entire period.

	ΔS	ΔL	ΔH	ΔLE
$z_{om}/10$	0.0	0.2	-5.9	-1.8
$z_{om} * 10$	0.0	-0.1	14.2	4.3
$S - 2\%$	-1.4	0.2	0.2	0.2
$L_{in} - 2\%$	0.0	-5.8	0.7	0.6
$L_{in} + 2\%$	0.0	6.2	-0.4	-0.4
$T_a + 1^{\circ}\text{C}$	0.0	-0.2	15.9	-1.1
$WSP + 20\%$	0.0	-0.1	7.2	2.3
$WHC = 0.0$	0.0	0.5	1.5	1.2
$WHC = 0.08$	0.0	0.0	-0.2	-0.2

A positive value indicates an additional flux towards the surface. The model parameters/meteorological variables that have been varied are: roughness length for momentum (z_{om}), net solar radiation (S), incoming longwave radiation (L_{in}), air temperature (T_a), wind speed (WSP) and water holding capacity of snow (WHC).

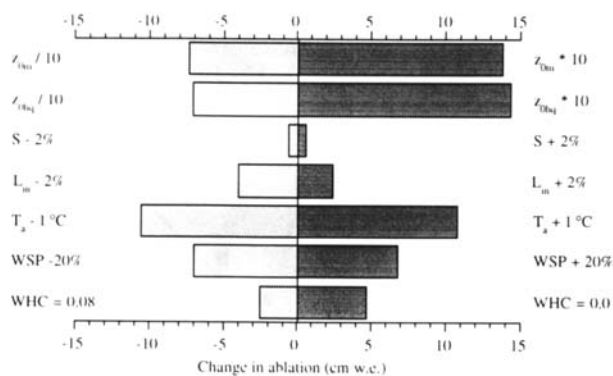


Fig. 15. Change in mean modelled ablation caused by variations made in model parameters and meteorological quantities (z_{om} = momentum roughness length, z_{ohq} = scalar (heat, moisture) roughness length, S = net shortwave radiation, L_{in} = incoming longwave radiation, T_a = air temperature, WSP = wind speed and WHC = water holding capacity of snow).

the same pattern as in Table III emerges since the sum of the additional surface fluxes provides the extra energy for ablation. Changes in the scalar roughness lengths have a comparable effect on the surface fluxes as changes in z_{om} . Allowing no water to stay inside the snow ($WHC = 0$) increases the ablation despite the lower surface temperatures. This is due to the fact that melted snow immediately runs off and does not stay inside the snow. A change in air temperature of 1°C results in a change of nearly 15% in the ablation. This is a large change, considering the fact that a 1°C change in air temperature is probably more likely to happen than, for instance, a 15% change in solid precipitation. It may be concluded that the Ecology Glacier is probably quite sensitive to changes in atmospheric temperature. It is likely that this conclusion applies more generally to other (nearby) glaciers and small ice caps located in comparably warm Antarctic climates.

Discussion and conclusions

Meteorological measurements were performed in the ablation zone of the Ecology Glacier, King George Island, Antarctica, during one month in the austral summer of 1990–91. King George Island is situated in the subantarctic westerly wind zone, which causes the climate to be relatively warm and humid. Mean summertime temperatures over the Ecology Glacier are well above zero ($+2.0^\circ\text{C}$). During periods with a small synoptic pressure gradient, occasional south-easterly winds originating from the Weddell Sea occur.

A model has been used to calculate the surface energy fluxes and ablation rates with input from meteorological quantities.

The model incorporates the calculation of the turbulent fluxes, subsurface temperatures, melt rates, density profiles and penetration of solar radiation in a physically plausible way. With an appropriate choice of the surface roughness

lengths, the model is able to simulate the observed ablation rate with good accuracy. The total ablation during the one-month measuring period is 73.5 cm w.e.

In the model simulations radiation provided most of the energy used for melting (64%), despite the large quantity of low clouds (0.83). An important feature is the large mean value of the incoming longwave radiation (305.5 W m^{-2}), which is due to the large amount of clouds and low mean cloud base. The turbulent heat fluxes supplied 36% of the energy used for melting, of which 29% is provided by the sensible heat flux and 7% by the latent heat flux.

The sensitivity analysis performed with the model demonstrates the relatively large sensitivity of the turbulent fluxes to variations in model variables and/or meteorological quantities. For instance, an increase in air temperature of 1°C enhances the ablation by 15%. If this number can be used to express changes in ablation due to climate change-related temperature changes (which may be approximately true), the Ecology Glacier is quite sensitive to changes in temperature. Presumably, this conclusion will also apply to glaciers and small ice caps located on the other South Shetland Islands and in the northern part of the Antarctic Peninsula since they are located in the same 'warm' climate. This means that a significant part of the Antarctic ice volume may be sensitive to short-term variations in climate, especially when one takes into account the fact that the marginal sea-ice zone around Antarctica is generally considered to be one of the regions most sensitive to climatic changes (Mitchell *et al.* 1990). Needless to say, this issue is of great importance for possible near-future sea-level changes.

Acknowledgements

I thank M.J. Portanger and L.A. Conrads for assistance during the field campaign and J. Oerlemans for his comments on an earlier version of the manuscript. Further I would like to thank all the members of the First Dutch Antarctic Expedition and of the 14th and 15th Polish Expedition at Arctowski Station for their help and support. Financial support was provided by the Netherlands Antarctic Research Programme (SOZ/GOA).

References

- AMBACH, W. 1974. The influence of cloudiness on the net radiation balance of a snow surface with high albedo. *Journal of Glaciology*, **13**, 73–84.
- BINTANJA, R. 1992. Glaciological and meteorological investigations on Ecology Glacier, King George Island, Antarctica (summer 1990–91). *Circumpolar Journal*, **7**, 59–71.
- BINTANJA, R., CONRADS, L.A., OERLEMANS, J. & PORTANGER, M.J. 1991. *Glacio-meteorological investigations on Ecology Glacier, summer 90–91, King George Island, Antarctica. Arctowski-90/91 Field Report*. (Available from: Institute for Marine and Atmospheric research Utrecht, Utrecht University, P.O. Box 80005, 3508 TA Utrecht, the Netherlands), 17 pp.
- BINTANJA, R. & VAN DEN BROEKE, M.R. 1995. Momentum and scalar transfer coefficients over aerodynamically smooth Antarctic surfaces. *Boundary-Layer Meteorology* (in press).

- BRUTSAERT, W.H. 1982. *Evaporation into the atmosphere*. Dordrecht: Reidel, 299 pp.
- CLAPPERTON, C.M. 1990. Quaternary glaciations in the Southern Ocean and Antarctic Peninsula area. *Quaternary Science Reviews*, **9**, 229-252.
- CLAPPERTON, C.M. & SUGDEN, D.E. 1988. Holocene glacier fluctuations in South America and Antarctica. *Quaternary Science Reviews*, **7**, 185-198.
- DUYNKERKE, P.G. 1991. Radiation fog: a comparison of model simulation with detailed observations. *Monthly Weather Review*, **119**, 324-341.
- GARRATT, J.R. & HICKS, B.B. 1973. Momentum, heat and water vapour transfer to and from natural and artificial surfaces. *Quarterly Journal of the Royal Meteorological Society*, **99**, 680-687.
- GREUILL, W. & OERLEMANS, J. 1987. Sensitivity studies with a mass balance model including temperature profile calculations inside the glacier. *Zeitschrift für Gletscherkunde und Glazialgeologie*, **22**, 101-124.
- HARSTVEIT, K. 1984. Snowmelt modelling and energy exchange between the atmosphere and a melting snow cover. *Geophysical Institute, Meteorological Division, University of Bergen, Scientific Report No. 4*.
- HOGG, I.G.G., PAREN, J.G. & TIMMIS, R.J. 1982. Summer heat and ice balances on Hodges Glacier, South Georgia, Falkland Island Dependencies. *Journal of Glaciology*, **28**, 221-238.
- HÖGSTRÖM, U. 1988. Non-dimensional wind and temperature profiles in the atmospheric surface layer: a re-evaluation. *Boundary-Layer Meteorology*, **42**, 55-78.
- HUYBRECHTS, P. & OERLEMANS, J. 1990. Response of the Antarctic ice sheet to greenhouse warming. *Climate Dynamics*, **5**, 93-102.
- MANABE, S. & STOFFER, R.J. 1980. Sensitivity of a global climate model to an increase of CO₂ concentration in the atmosphere. *Journal of Geophysical Research*, **85**, 5529-5554.
- MARTIANOV, V. & RAKUSA-SUSZCZEWSKI, S. 1989. Ten years of climate observations at the Arctowski and Bellingshausen Station (King George Island, South Shetlands, Antarctica). In BREYMEYER, A., ed. *Global Change Regional Research Centres: Scientific Problems and Concept Developments*, Warsaw, 80-87.
- MCCLATCHY, R.A., FENN, R.W., SELBY, J.E., VOLTS, F.E. & GARING, J.S. 1971. *Optical properties of the atmosphere*. 3rd ed, AFCRL-72-0497.
- MITCHELL, J.F.B., MANABE, S., TOKIOKA, T. & MELESHKO, V. 1990. Equilibrium climate change. In HOUGHTON, J.T., JENKINS, G.J. & EPHRAUMS, J.J., eds. *Climate Change: The IPCC Scientific Assessment*. Cambridge: Cambridge University Press, 131-172.
- OERLEMANS, J. 1992. Climate sensitivity of glaciers in southern Norway: application of an energy-balance model to Nigaardsbreen, Hellstugubreen and Alftobreen. *Journal of Glaciology*, **38**, 223-232.
- ORHEIM, O. & GOVORUKHA, L.S. 1982. Present-day glaciation in the South Shetland Islands. *Annals of Glaciology*, **3**, 233-238.
- PARISH, T.R. 1983. The influence of the Antarctic Peninsula on the wind field over the western Weddell Sea. *Journal of Geophysical Research*, **88**, 2684-2692.
- PATERSON, W.S.B. 1981. *The physics of glaciers*. Oxford: Pergamon Press, 380 pp.
- SCHWERDTFEGER, W. 1984. *Weather and climate of the Antarctic*. Amsterdam: Elsevier Science Publishers, 261 pp.
- ZAMORUYEV, V.V. 1972. Results of glaciological observations at 'Bellingshausen' station in 1968. *Trudy Sovetskoy Antarkticheskoy Ekspeditsii*, **55**, 135-144 [in Russian.]